Photochemistry and Photobiology, 2010, 86: 871–881

Ultraviolet Radiation Induces Filamentation in Bacterial Assemblages from North Andean Patagonian Lakes

Beatriz Modenutti*[1], Esteban Balseiro[1], Gianluca Corno[2,3], Cristiana Callieri[2], Roberto Bertoni[2] and Emanuele Caravati[2]

[1]Laboratorio de Limnología, INIBIOMA (CONICET-UNComahue), Quintral 1250, Bariloche, Argentina
[2]CNR, Institute of Ecosystem Study, Verbania Pallanza, Italy
[3]Limnological Station, Institute of Plant Biology, University of Zurich, Kilchberg, Switzerland

Received 12 February 2010, accepted 11 April 2010, DOI: 10.1111/j.1751-1097.2010.00758.x

ABSTRACT

Through laboratory experiments, we tested whether UV radiation (UVR) induces filamentation in natural bacteria assemblages from North Andean Patagonian lakes. We incubated water from three different lakes for 72 h in four separate treatments: (1) UVR + PAR (photosynthetically active radiation), (2) 50% UVR + PAR, (3) PAR and (4) 50% PAR. The irradiance levels used in the experiments were equivalent to those registered at the epilimnion of the lakes. In the UVR treatments filamentation was induced after the first 24 h and the proportion continued to increase for the next 48–72 h. A comparison of the gross composition and diversity of the entire community (cells >0.2 μm) with bacterial filaments alone (>5.0 μm) showed that UVR-induced filamentation is not a feature of any particular cluster. By sequencing part of the 16S rRNA gene of the taxonomic units obtained using denaturing gels, we observed that strains in the *β-Proteobacteria* group were of relatively high importance in filament formation, followed by *Cytophaga–Flavobacterium–Bacteroides*, *γ-Proteobacteria* and *α-Proteobacteria*, whereas *Actinobacteria* were almost nonexistent in the filaments. We propose that UVR doses equivalent to those of Andean lakes produce bacterial morphological changes, and that all bacterial groups except *Actinobacteria* can potentially form filaments.

INTRODUCTION

Filamentation is one of the most studied phenotypic antipredation strategies against protists in aquatic environments, and filamentous bacteria are a conspicuous and ecologically distinct component of many freshwater systems (1,2). Filaments have been observed to form permanent planktonic populations in hypertrophic lakes (3). These morphotypes are also reported to be very active and abundant in an oligotrophic high mountain lake and in various anthropogenically acidified Czech lakes (4–6). In natural environments, the presence of large predators (zooplankton) may reduce the effectiveness of filamentation as an antipredation strategy, because these predators directly ingest filaments and prey on nanoflagellates (7,8). Predatory activity by nanoflagellates, in laboratory experiments, has been found to have an indirect positive effect in extremely oligotrophic systems, resulting from the release of large amounts of soluble exudates during grazing (9). Consequently, predation should help maintain bacterial diversity in systems highly limited by nutrient availability (10).

Although filamentation is an effective strategy in resisting grazing by nanoflagellates (9), other environmental factors have also been found to stimulate filament formation (11,12). In particular, early studies of *Escherichia coli* (13,14) and, more recently, *Vibrio angustum* S14 strains (15) indicate that exposure to UV radiation (UVR) provokes the formation of filamentous cells. Recent experimental studies on the filamentous cyanobacterium *Arthrospira platensis* indicated that its morphology is substantially modified by solar UVR (16). UVR inhibits septum formation in *E. coli* K-12 as a result of alterations in DNA metabolism (17). However, there is evidence indicating that filamentation does not involve permanent mutation; cell division is inhibited until repair mechanisms are activated, but once DNA repair is complete, the capacity for cell division is restored (18).

The promotion of bacterial filamentation by UVR was only observed in laboratory strains, with no analogous findings in natural bacterial assemblages. However, as part of our studies of ultraoligotrophic clear Andean lakes with high UVR, we observed that filamentous bacterial cells were heterogeneously distributed in the upper levels of the water column (19). Our data suggest that UVR could be, in nature, implicated in promoting bacterial filamentation. There is growing information about the different sensitiveness of bacterial groups to UVR impact; therefore, bacteria diversity can be also influenced by UVR. In laboratory experiments, *Sphingomonas* sp. strain RB2256, a facultative oligotrophic ultramicrobacterium, exhibited little DNA damage and a high level of UV-B resistance (20). In nature, a high resistant bacterial community was observed in a high altitude lake form the northwestern Argentinean Andes (21). In the Mediterranean Sea it was observed that naturally dominating phylogenetic bacterial groups have different sensitivity to natural levels of incident solar radiation: members of the *γ-Proteobacteria* and *Bacteroidetes* groups appeared to be highly resistant to solar radiation, while *α-Proteobacteria* were more sensitive to

*Corresponding author email: bmodenutti@comahue-conicet.gob.ar (Beatriz Modenutti)

radiation (22). More recently, a UVR-resistant phylotype affiliated to *Erythrobacter* sp. (previously designated as *Sphingomonas* sp.) was reported from warmer waters in the Pacific Ocean (23).

Therefore, the purpose of the present study was to determine experimentally whether UVR favors large filament morphologies in natural microbial communities and investigate its influence on bacterial diversity. To address these topics, we carried out laboratory experiments to study how filamentation and genetic diversity respond to natural levels of irradiance.

MATERIALS AND METHODS

Study area. The studied lakes are located around 41°S in the North Andean Patagonia region (Argentina), corresponding to the glacial lake district of the Southern Andes. Laboratory experiments involving three lakes were carried out: Lakes Correntoso and Gutiérrez (Nahuel Huapi Basin) in the Atlantic watershed and Lake Mascardi Catedral (Manso Basin) in the Pacific watershed, all located at 750 m above sea level. The lakes exhibit a warm monomictic thermal regime, with thermal stratification in late spring and summer. Photosynthetically active radiation (PAR) and UVR penetration is high (45 m for PAR and 17 m for the 340 nm band of UVR), while dissolved organic carbon (DOC) and phosphorus concentrations are very low (DOC$\sim$0.6 mg L^{-1}; TP $<$ 4 μg L^{-1}) (24,25).

Samples for laboratory experiments were obtained within the euphotic zone at 20 m depth, approximately 1% of UV 340 nm band, and a temperature of 15 ± 1°C (determined with a PUV 500B submersible radiometer; Biospherical Instruments). Experiments were carried out in late spring: November 2008 (Lakes Gutiérrez and Mascardi) and December 2008 (Lake Correntoso).

Experimental design. Effect of filtration and cycloheximide on nanoflagellates. We carried out a preliminary experiment to test the effects of filtration (5 μm pore size) and the addition of a very low concentration of a eukaryotic inhibitor (cycloheximide, 100 μg L^{-1} final concentration) in reducing nanoflagellates. This low concentration of cycloheximide (MW of $C_{15}H_{23}NO_4$ = 281.4; SIGMA C1988-1G) was chosen because it implies an increase of only 10% (0.064 mg C L^{-1}) from the original DOC concentration of the lake (DOC = 0.6 mg L^{-1}). DOC was determined using a Shimadzu TOC 5000 carbon analyzer before and after the addition of cycloheximide in a previous and separate experiment, and no significant differences were found (*t*-test $P > 0.05$, d.f. = 4).

Water (4 L) from Lake Gutiérrez was collected at a depth of 25 m; 60 mL was fixed in filtered (0.2 μm) formaldehyde solution (2% vol/vol) for nanoflagellate quantification. A volume of 1500 mL was immediately filtered through a 5 μm pore size filter (polycarbonate Millipore). This volume was distributed in six 250 mL quartz containers, which were then placed in a device that half-rotates the bottles every 2 min. Cycloheximide (100 μg L^{-1} final concentration) was added to half of the containers. All containers were kept for 12 h under experimental conditions (15 ± 1°C and 12L:12D photoperiod of daylight fluorescent tubes = 92 μmol m^{-2} s^{-1} PAR); this time was considered the start of the preliminary experiment (T_0). The containers were then incubated under the same conditions for 72 h (T_{72}). At T_0 and T_{72}, a volume of 40 mL of each replicate was fixed in filtered (0.2 μm) formaldehyde solution (2% vol/vol). Nanoflagellate enumeration was performed on 1 μm polycarbonate black membrane filters by staining with fluorochrome 4′,6-diamidino-2-phenylindole (DAPI; final concentration 2% vol/vol) (26). Cells were counted *via* epifluorescence microscopy at 1250× magnification, using both UV and blue light, to distinguish heterotrophic nanoflagellates (HNF) from mixotrophic nanoflagellates.

Most of the flagellates (>90%) were mixotrophic species larger than 5 μm, such as *Chrysochromulina* sp. (the most abundant group), which is 6.8 μm in average diameter. HNF (5 μm in average diameter) were present in a very low proportion (5–8%). This preliminary experiment (Table 1) showed that filtration causes a significant reduction in nanoflagellate abundance, and that the addition of cycloheximide (100 μg L^{-1} final concentration) enhanced the reduction and prevents growth over the next 72 h. Therefore, we used a combination of these two methods in our experiments.

Table 1. Nanoflagellate abundance in samples of unfiltered water from Lake Gutiérrez (Field), filtered through 5 μm, at two different experimental times (T_0 and T_{72}) with and without the addition of cycloheximide (100 μg L^{-1}).

Field	Treatments	T_0	T_{72}
1430 ± 34.7	Without cycloheximide	261 ± 9.67 (82%)	106 ± 8.66 (92%)
	With cycloheximide	126 ± 7.65 (91%)	39 ± 1.41 (97%)
Statistical results *t*-test	d.f. = 4	$P < 0.001$	$P = 0.002$

Data are means ± standard error. In brackets are the percentages of nanoflagellate reduction, in comparison to field abundance.

Filamentation experiments. Lake water (Lakes Correntoso, Gutiérrez and Mascardi) was filtered through 5 μm filters (polycarbonate Millipore) to eliminate large predators and then treated with cycloheximide (100 μg L^{-1} final concentration), as explained above, for 12 h under experimental conditions (15 ± 1°C and 12L:12D photoperiod of daylight fluorescent tubes = 92 μmol m^{-2} s^{-1} PAR). The water was then diluted (1:1) with freshly filtered lake water (cellulose acetate sterile filters, 0.2 μm). The potential contribution of DOC from the 0.2 μm filter used was previously checked by comparing filtered and unfiltered MilliQ water. We observed no difference and concluded that using the filters does not increase the DOC concentration (*t*-test $P > 0.05$, d.f. = 4). The water was examined under light and epifluorescence microscopy for any potential growth of nanoflagellates; in all experiments, nanoflagellates were undetectable (97% reduction, Table 1). All glassware used in the various procedures was previously sterilized (autoclaved for 30 min). A volume of 100 mL of water (from the field, and treated with the laboratory procedures outlined above) was filtered onto a precombusted GF/F filter for DOC, dissolved phosphorus and spectrophotometric scan analyses. DOC was measured with a Shimadzu TOC 5000 carbon analyzer and dissolved phosphorus was determined *via* the ascorbate-reduced molybdenum method. Additionally, spectrophotometric scans (250–800 nm) were performed to assess changes in the relative size of dissolved organic matter (DOM) due to UVR (27).

The experiment began when the water (treated with cycloheximide and then diluted) was distributed in 12 250 mL quartz containers that were placed in a device that half-rotates the containers every 2 min; this time was considered T_0. We performed four treatments with three replicates each: (1) exposed to UVR + PAR, (2) exposed to 50% UVR + PAR, (3) exposed to PAR and (4) exposed to 50% PAR. Experiments were carried out in an incubator at 15 ± 1°C with a 12L:12D photoperiod and PAR intensity of 92 μmol m^{-2} s^{-1} (daylight fluorescent tubes). The UVR source was provided by two UVA-340 fluorescent tubes (Q-Panel Lab Products, Cleveland, OH). UVR exposure lasted 4 h each day, centered in the 12 h of PAR exposure. The UV spectrum of these tubes closely resembles the solar spectrum (between 280 and 350 nm) (28). Throughout UVR incubation, the water received 30 μW cm^{-2} nm^{-1} of the 340 nm band and 7 μW cm^{-2} nm^{-1} of the 305 nm band of UV-B, this being an irradiance level equivalent to surface noon summer sunlight in Andean lakes (19,24). The 50% PAR and 50% UVR + PAR treatments were obtained using neutral screening that lowered the PAR intensity to 48 μmol m^{-2} s^{-1}, and the UVR 340 nm band to 15 μW cm^{-2} nm^{-1}, and the 305 nm band to 3 μW cm^{-2} nm^{-1}.

The experiments lasted 72 h, and samples (40 mL) for determining bacterial abundance and morphology and for genetic identification were collected at the start of the experiment (T_0) and after 24 h (T_{24}), 48 h (T_{48}) and 72 h (T_{72}) of incubation. At each sampling time, the volume of 40 mL was replaced with lake water filtered through a sterile 0.2 μm filter (cellulose acetate sterile filters).

UVR–cycloheximide interaction experiment. We carried out an additional experiment to test the possible interaction between the effects of UVR and cycloheximide on bacterial filamentation. Water

(4 L) from Lake Gutiérrez was collected at a depth of 25 m and immediately filtered through a 5 μm pore size filter (polycarbonate Nucleopore). Half of this volume was treated with cycloheximide (100 μg L^{-1} final concentration). After 12 h (T_0) under experimental conditions (15 ± 1°C and 12L:12D photoperiod), the water (with and without cycloheximide) was distributed in 18 250 mL quartz containers. We performed the following treatments with three replicates each: (1) with or without the addition of cycloheximide and exposed to UVR + PAR, (2) with or without the addition of cycloheximide and exposed to PAR, (3) with or without the addition of cycloheximide and DARK (wrapped with aluminum foil). Light conditions and doses were the same as in the filamentation experiments. After 72 h (T_{72}) under experimental conditions, a volume of 40 mL of each replicate was fixed in filtered (0.2 μm) formaldehyde solution (2% vol/vol) for bacterial quantification.

Bacterial quantification. Samples for bacterial quantification were preserved in a filtered (0.2 μm) formaldehyde solution (2% vol/vol). Total bacterial enumerations were performed by staining with fluorochrome DAPI (final concentration 2% vol/vol) (26) on polycarbonate black membrane filters (0.2 μm pore size; Nucleopore) at 1250× magnification in an Olympus BX50 epifluorescence microscope using UV light. Different bacterial morphologies were distinguished (free living cocci and rods *vs* filamentous forms). When bacteria developed filamentous forms (> 7 μm), they were recorded as filaments that could be considered resistant to predation by nanoflagellates (29). A minimum of 500 total bacteria per sample was counted and processed using an image analysis system (Image-Pro Plus; Media Cybernetics). Filaments were manually measured using the image analysis system and biovolume was calculated as a cylinder (length of filaments × (1/2 width)^2 × π).

DNA extraction and amplification. Two water samples (10 mL each) from each treatment were taken at the beginning of the experiment (T_0) and at the end (T_{72}). Bacterial cells were collected selectively on Nucleopore® filters of 0.2 μm pore size (bacterial whole community, BT_0 and BT_{72}) or on Nucleopore® filters of 5.0 μm pore size (bacterial filaments, FT_{72}), both 25 mm in diameter. Nucleopore® filters were then collected and stored at −20°C in PBS, and transported to the Consiglio Nazionale delle Ricerche-Institute of Ecosystem Study (CNR-ISE) laboratories. DNA was then extracted from the filters using Ultraclean® Soil Isolation kits (MoBio), following the producer protocol for high yields, and dissolved in 30 μL TE (Tris-EDTA) buffer. Aliquots (1–2 μL) of extracted DNA were applied to the following mix to give a 50 μL PCR reaction mixture: 25 μL of GoTaq® Mastermix (Promega), 0.5 μL bovine serum albumin, 1 μL of the forward primer 357F-GC (a 40-base pair GC-clamp was added in position 5′), and 1 μL of an equal mixture of the reverse primers 907R and 907Rm, all 10 μmol L^{-1} concentrated. These primers were selected according to Sanchez *et al.* (30) for being the most sensitive and least subject to error in estimating the diversity of aquatic bacteria. PCR details are: initial denaturation at 96°C for 5 min, amplification using 10 touch-down cycles including denaturation at 94°C for 45 s, annealing at 65°C for 45 s decreased by 1°C for each cycle, and extension at 72°C for 2 min. This was followed by 20 additional cycles of denaturation at 94°C for 45 s, annealing at 55°C for 45 s, extension at 72°C for 2 min and a final elongation step at 72°C for 5 min (31). PCR products from the replicates were pooled and then purified with QIAquick PCR purification kits (Qiagen). Lastly, they were stored at −20°C until DGGE runs were performed.

Analysis by denaturating gradient gel electrophoresis (DGGE). DGGE was performed using a Dcode™ instrument and a gradient former model 475, according to the manufacturer's instructions (Bio-Rad). The denaturing gradient was formed using two 9% acrylamide (acrylamide-bis 37.5:1) stock solutions (Promega) in 1× TAE (20 mM Tris, 10 mM acetate, 0.5 M EDTA, pH 7.4). The 100% denaturant solution contained 40% formamide and 7 M urea. Perpendicular DGGE analyses were carried out in order to select appropriate electrophoresis conditions: the gels were then made with denaturing gradients ranging from 35% to 60%. A volume of 13 μL of purified PCR products was mixed with 3 μL loading dye before loading. Gels were run in 1× TAE at 60°C for 16 h at 90 V and stained with SYBR Green I Nucleic Acid Gel Stain (Cambrex) for 30 min. Digitized DGGE images from the high-resolution UV illuminator Gel DOC XR system (Bio-Rad) were analyzed with Quantity One software (Bio-Rad). Bands occupying the same position in the different lanes of the gels were identified.

A density profile through each lane was established, the bands detected (regarded as operational taxonomic units [OTUs]) and the relative contribution of each band to the total band signal was calculated in the lane after applying a rolling disk as background subtraction. Bands with a relative intensity of < 0.5% of the total intensity of the lane were disregarded. Remaining bands considered as valid bands were used to assess the relative gross diversity of each sample.

Sequencing of selected DGGE bands. All dominant bands were excised from the DGGE gels with a sterile scalpel, placed in 50 μL sterile water and incubated at 4°C overnight to permit diffusion of DNA into the water. One microliter of each solution containing excised bands was re-amplified using the same primers and the same PCR conditions described above, except the 357F primer was used without a GC-clamp. PCR products were purified using a QIAquick PCR purification kit (Qiagen) in order to remove dimers, which were occasionally produced. Part (3 μL) of the PCR product was run on a 0.8% high-quality agarose gel to check the purity and confirm the melting behavior of the excised band. The inserts (*ca* 550bp) recognized as pure were sequenced by Macrogen (Korea) using primer 357F.

Data analysis. The results of each of the three filamentation experiments were analyzed with two-way repeated measurement ANOVAs (RMANOVA) (*i.e.* Lake Mascardi, Lake Gutiérrez and Lake Correntoso). For each analysis, the between-subjects factor was light treatments (UVR + PAR, 50% UVR + PAR, PAR and 50% PAR) and the within-subjects factor was time (T_0, T_{24}, T_{48} and T_{72}). The variables analyzed were filament number and average length of filaments. Normality, homoscedasticity and sphericity assumptions were previously verified. Greenhouse-Geisser's statistics was used to compute adjusted *P*-level of *F*-test. *A posteriori* multiple comparisons Tukey test was applied to determine significant differences between treatments and times. Statistical analyses were carried out with SPSS 18.

The results of the UVR–cycloheximide interaction experiment carried out in Lake Gutiérrez was analyzed with a two-way analysis of variance (two-way ANOVA). The factors considered in this analysis were light source (UVR + PAR, PAR, DARK) and cycloheximide (with or without the addition of cycloheximide). The variables considered were number of filaments and proportion of filament biovolume to total biovolume. *A posteriori* multiple comparison Tukey test was applied to determine significant differences between treatments. Normality and homoscedasticity assumptions were previously verified. Statistical analyses were carried out with Sigma Stat 3.5.

The gross diversity and relative composition in OTUs of the bacterial communities within different treatments and at various times were assessed by analyzing the DGGE profiles and the sequences obtained by sequencing excised bands. The Shannon diversity index (H) was calculated by using single peaks as OTUs.

$$H = -\sum_{i=1}^{s} p_i \ln p_i$$

where $p_i = n_i/N$, in our case n_i = OTU_i and N = total value of OTU peak heights.

Peak heights were standardized through the profile in order to reduce the impact of the background signal on the profile, using the software Quantity One (Bio-Rad). In our case the standardization did not significantly change any proportion or trend, confirming the good quality of our gels and the replicability of our profiles.

Similarities between initial time (T_0) and T_{72} in the different treatments were assessed with the Jaccard similarity index (32) with the presence/absence of different OTUs.

RESULTS

At the beginning of the filamentation experiments, the proportion of filament numbers was below 0.9% (0.91% in Lake Gutiérrez, 0.82% in Lake Correntoso and 0.78% in Lake Mascardi). However, during the 3 days of experimentation, a significant increase in the number of filaments was recorded in

the UVR (full and 50%)-exposed treatments in all experiments (two-way RMANOVA $P < 0.001$ in each of the three experiments) (Fig. 1, Table 2). In addition, the average length of filaments increased in treatments exposed to UVR (two-way RMANOVA $P < 0.001$ in Correntoso and Gutiérrez and $P < 0.01$ in Mascardi) (Fig. 1, Table 2). The maximum increase in filament length was observed in Gutiérrez, where filaments reached a length of 100 μm in the 50% UVR + PAR treatment. Consequently, the bacterial assemblages in UVR-exposed treatments exhibited a different morphology/size distribution, with larger cells tending to become relatively more significant in terms of filament abundance and biomass (Fig. 1).

Bacterial abundances at the beginning of the three experiments (T_0) were 5.6×10^5 cell mL^{-1} in Correntoso, 4.0×10^5 cell mL^{-1} in Gutiérrez, and 6.7×10^5 cell mL^{-1} in Mascardi. Positive bacterial growth rates were recorded for all three experiments. As a consequence of the observed changes in filament abundance and length (Fig. 1, Table 2), biovolume varied in the different treatments, being higher in the UVR-exposed treatments.

DOC concentration in all three lakes was always very low, around 50 μM (0.6 mg L^{-1} ± 0.03 in Lake Mascardi, 0.6 mg L^{-1} ± 0.06 in Lake Correntoso and 0.6 mg L^{-1} ± 0.04 in Lake Gutiérrez). Spectrophotometric scans of the water indicated no significant changes in the relative size of DOM during incubation. Dissolved phosphorus was under 0.09 μM.

No interaction between cycloheximide (100 μg L^{-1}) and UVR was observed in the outcome of bacteria filamentation, as no statistical differences between treatments with and without cycloheximide were found (Fig. 2, Table 3). Nevertheless, significant differences were observed between the treatments exposed to UVR and those that were not (PAR and DARK) (Fig. 2, Table 3). We can therefore conclude that the use of such a low concentration of cycloheximide does not induce filamentation by itself or through an interaction with UVR.

Bacterial diversity

In Lake Correntoso at T_0 (BT_0), 26 DGGE bands (OTUs) were detected ($H = 3.18$), while Lake Gutiérrez had 19 OTUs ($H = 2.73$) and Lake Mascardi only 17 OTUs ($H = 2.65$). At

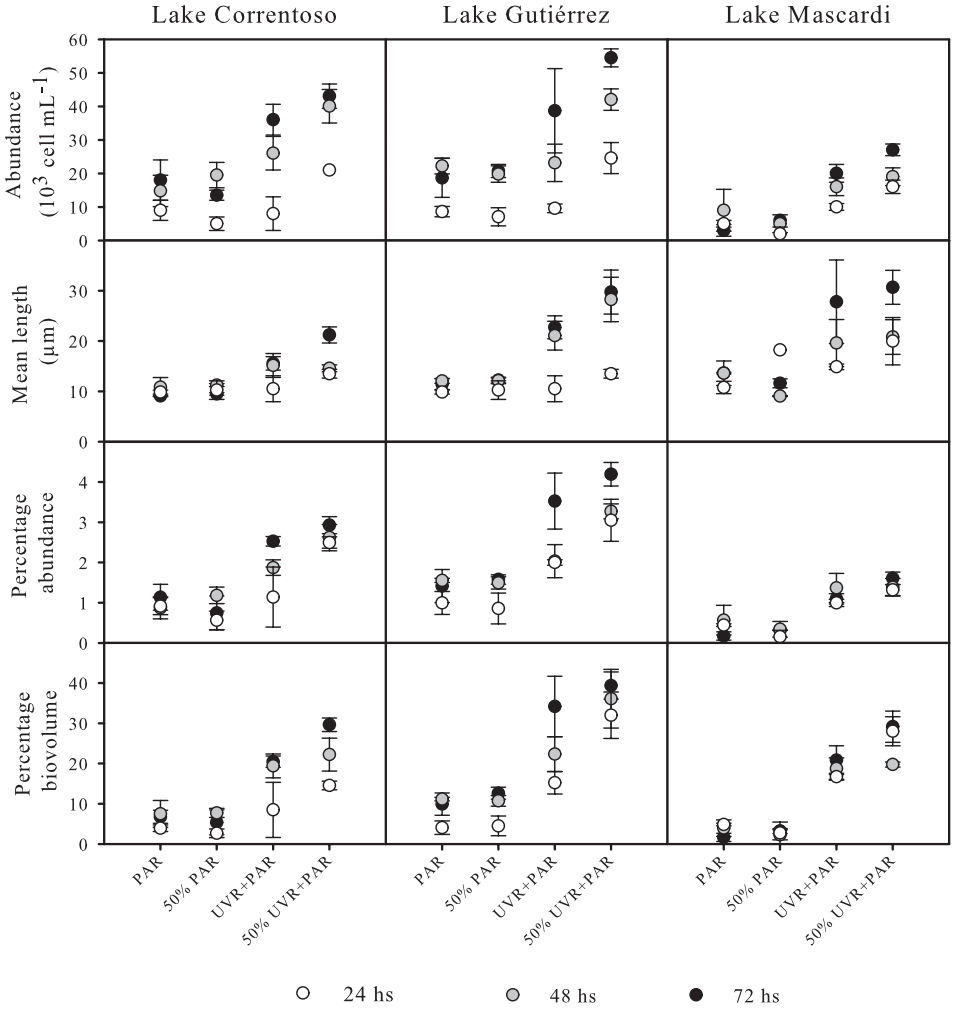

Figure 1. Results of the laboratory experiments (Lakes Correntoso, Gutiérrez and Mascardi). First row: filament abundance; second row: filament length (mean length of cell > 7 μm); third row: percentage of filaments to total cell abundance; fourth row: percentage of filament biovolume to total cell biovolume. Treatments: PAR, 50% PAR, UVR + PAR, 50% UVR + PAR. Exposure time (bar color): white = T_{24}; gray = T_{48}; black = T_{72}. Values are given as average ± standard error.

Table 2. Results of the RMANOVA of the filamentation experiments in Lakes Correntoso, Gutiérrez and Mascardi. *P** is the adjusted probability calculated based on Epsilon of Greenhouse-Geisser when sphericity assumption is not met (Mauchly's test $P < 0.05$).

Correntoso filament number

Sphericity Mauchly's test

Mauchly's test *W*	d.f.	*P*	Epsilon Greenhouse-Geisser
0.313	2	0.017	0.593

Source of variation	d.f.	SS	MS	*F*	*P**
Light treatment	3	2760572843	920190947	12.65	0.0016
Individuals	8	589239758	73654969		
Time	2	1704107508	852053754	27.22	0.0001
Light × time	6	553233185	92205530	2.94	0.0854
Residual	16	438096416	31292601		
Total	35	6279059204	190274521		

Gutiérrez filament number

Sphericity Mauchly's test

Mauchly's test *W*	d.f.	*P*	Epsilon Greenhouse-Geisser
0.673	2	0.250 NS	–

Source of variation	d.f.	SS	MS	*F*	*P*
Light treatment	3	3507533208	1169177736	11.83	0.0026
Individuals	8	790791814	98848977		
Time	2	2694397815	1347198907	22.95	0.00002
Light × time	6	580662406	96777068	1.65	0.198
Residual	16	939231783	58701986		
Total	35	8512617026	243217629		

Mascardi filament number

Sphericity Mauchly's test

Mauchly's test *W*	d.f.	*P*	Epsilon Greenhouse-Geisser
0.673	2	0.250 NS	–

Source of variation	d.f.	SS	MS	*F*	*P*
Light treatment	3	1660979186	553659729	25.11	0.0002
Individuals	8	176422653	22052832		
Time	2	209000700	104500350	5.18	0.018
Light × time	6	220027116	36671186	1.82	0.158
Residual	16	322773264	20173329		
Total	35	2589202920	73977226		

Correntoso filament length

Sphericity Mauchly's test

Mauchly's test *W*	d.f.	*P*	Epsilon Greenhouse-Geisser
0.621	2	0.188 NS	–

Source of variation	d.f.	SS	MS	*F*	*P*
Light treatment	3	217.21	72.40	16.070	0.0007
Individuals	8	35.37	4.42		
Time	2	36.34	18.17	2.208	0.1467

Table 2. Continued

Correntoso filament length					
Sphericity Mauchly's test					
Source of variation	d.f.	SS	MS	*F*	*P*
Light × time	6	96.22	16.04	1.949	0.1424
Residual	16	115.22	8.23		
Total	35	520.21	15.76		
Gutiérrez filament length					
Sphericity Mauchly's test					
Mauchly's test *W*	d.f.	*P*		Epsilon Greenhouse-Geisser	
0.961	2	0.869 NS		–	
Source of variation	d.f.	SS	MS	*F*	*P*
Light treatment	3	1415.26	471.75	8.024	0.0085
Individuals	8	470.32	58.79		
Time	2	17.38	8.69	1.268	0.3081
Light × time	6	29.08	4.85	0.707	0.6485
Residual	16	109.64	6.85		
Total	35	2041.67	58.33		
Mascardi filament length					
Sphericity Mauchly's test					
Mauchly's test *W*	d.f.	*P*		Epsilon Greenhouse-Geisser	
0.940	2	0.805 NS		–	
Source of variation	d.f.	SS	MS	*F*	*P*
Light treatment	3	560.50	186.83	3.765	0.0478
Individuals	8	410.56	51.32		
Time	2	135.59	67.80	1.711	0.2121
Light × time	6	247.06	41.18	1.039	0.4367
Residual	16	435.80	39.62		
Total	35	2206.15	73.54		

$T_{72,}$ the overall richness was 24 for Correntoso, 18 for Gutiérrez and 18 for Mascardi, and H ranged between 3.06 and 2.89, without any significant differences observed among the treatments (one-way ANOVA $P = 0.935$ for richness and $P = 0.982$ for H) or lake of origin (one-way ANOVA $P = 0.069$ for richness and $P = 0.068$ for H).

The similarity index based on the presence or absence of the different OTUs at T_0 and T_{72} showed only slight differences (Table 4). The Jaccard index was always higher than 0.8, except in the treatments from Lake Mascardi at T_0, suggesting that different light treatments did not substantially affect community composition (Table 4).

Bacterial community composition

Sequencing bands excised from DGGE gels allowed us to determine between 85% and 100% of the biodiversity detected (as by DGGE bands). All major bacterial groups were detected by our analyses. If we consider the OTUs with major contributions (more than 3%) in Lakes Correntoso and Gutiérrez, only slight differences in community composition were observed between T_0 and T_{72}. After the 72 h of experimentation in the UVR treatment, only a few OTUs were lost (B39 in Lake Gutiérrez and B35 in Lake Correntoso). In Lake Mascardi after 72 h, no OTU loss was observed, although we did record an increase in the relative importance of three *β-Proteobacteria* (B33, B25 and B13) (see BT_0 and BT_{72} of each lake in Fig. 3).

The only *γ-Proteobacteria* (90% identity with *Nevskia* sp. AB426558 with 99% coverage of the DNA fragment) was found in samples from Lake Correntoso, and it accounted for about 5% of the total DGGE signal of the related bands; its relative proportion was constant in all treatments, with no differences between T_0 and T_{72} (Fig. 3).

Actinobacteria were present in all samples, both at T_0 and T_{72}. In general, five different bands were recognized; unfortunately the limited size of the excised fragment did not allow further assessments concerning species association. Their

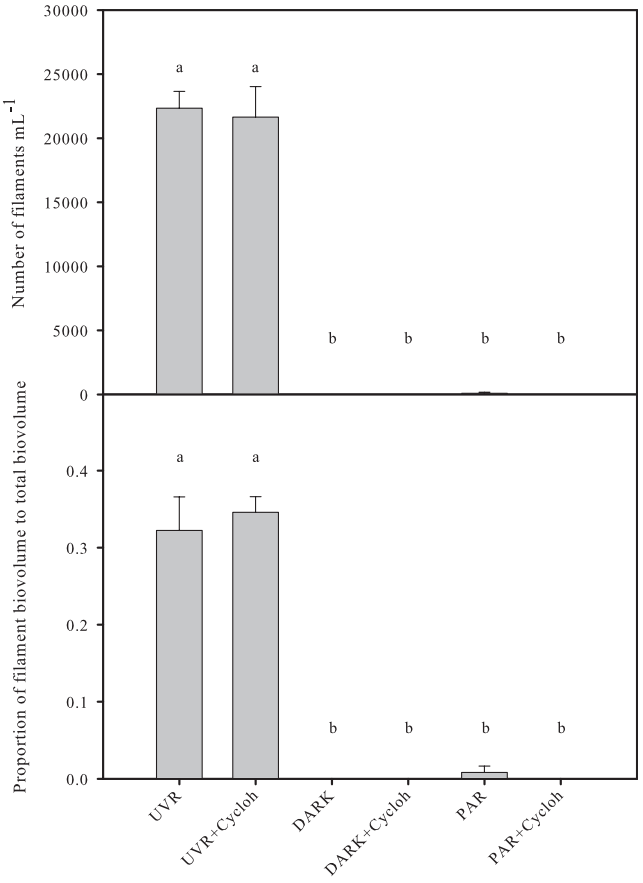

Figure 2. Number of filaments and proportion of filament biovolume to total biovolume in the UVR–cycloheximide interaction experiment (Lake Gutiérrez) after 72 h of incubation (T_{72}). Treatments: UVR, UVR + Cycloheximide, DARK, DARK + Cycloheximide, PAR, PAR + Cycloheximide. Values are given as average ± standard error. Lower case letters in the graphs indicate homogeneous groups from the *a posteriori* Tukey test.

Table 3. Two-way ANOVA results of the UVR–cycloheximide interaction experiments.

Source of variation	d.f.	*F*	*P*
Variable: Filament number			
Light	2	178.08	< 0.001
Cycloheximide	1	0.57	0.465
Light × cycloheximide	2	0.22	0.803
Residual	12		
Total	17		
Variable: Proportion of filament biovolume to total biovolume			
Light	2	61.25	< 0.001
Cycloheximide	1	1.39	0.261
Light × cycloheximide	2	1.71	0.221
Residual	12		
Total	17		

relative proportion was higher in the bacterial community of Lake Correntoso (about 14% at T_0, reduced to 6–10% at the end of the experiment) and lower in the other lakes: 4–7% in Gutiérrez (Fig. 3) and ~3% in Mascardi (not shown in Fig. 3 because of the low proportion).

A total of six different bands of α-*Proteobacteria* were recognized. Their presence was generally lake-specific, but the relative proportion of α-*Proteobacteria* was always significant: about 5% in Lake Gutiérrez samples, rising to 10% in Lake Mascardi and to 25–30% of the signal for the entire DGGE profile of Lake Correntoso. The most important bands were very similar to *Brevundimonas* sp. (AB426562) and *Sphingomonas* spp. (accession numbers EU741013 and FJ626798).

Cyanobacteria were found (two bands) in the Lake Gutiérrez treatments (*Cyanobium* sp.) only at T_0, and in all samples and treatments from Lake Correntoso and Lake Gutiérrez, although in very small proportions (6% in Gutiérrez and 2–3% in Correntoso).

The *Cytophaga–Flavobacterium–Bacteroides* (CFB) group was very well represented in all samples, with important percentages (40–50% in Gutiérrez, 25–30% in Mascardi, 16–18% in Correntoso), and many different bands were recognized (14). OTUs with high degrees of similarity (up to 98%) to *Candidatus Aquirestis calciphila* strains (accession numbers: AJ786331, AJ786335) were common in samples from Lakes Gutiérrez and Mascardi.

β-*Proteobacteria* was the most important and diverse group, represented by 17 OTUs accounting for about 45%, 55% and 30% of the total profile signal in Lakes Gutiérrez, Mascardi and Correntoso, respectively. Single strains belonging to taxa in the Comamonaceae order showed a slight increase from T_0 to T_{72}, especially in Lake Mascardi.

Filament genetic composition

Analyses of filament genetic composition were performed on samples filtered through 5 μm filters at 72 h (FT_{72}). Based on FT_{72} samples, we were able to evaluate the relative importance of bacterial forms larger than 5 μm: filaments and cell aggregates. The proportion of aggregates was low in the natural samples (data not presented) and in the treatments at T_0 and at T_{72} (aggregates less than 3% of filaments in all samples). In the DGGE profiles measured at T_{72} under UVR in the samples filtered through a 5 μm filter, the overall richness of this large fraction of the assemblage dropped by 40–50% (see FT_{72} for each lake in Fig. 3). The number of significant bands ranged from 9 (Lake Mascardi) to 14 (Lake Correntoso). Many of the prominent bands dominating the bacterial community disappeared, while some others gained in relative importance (Fig. 3).

The γ-*Proteobacteria* band was found within the filament samples at a proportion similar to that of bacteria samples filtered through a 0.2 μm filter. *Actinobacteria* were almost absent in the samples used for filament analysis, except in Lake Gutiérrez. The α-*Proteobacteria* band was also found within the filament analysis samples, and was more significant in samples from Lake Correntoso. The relative proportion of CFB in the 5 μm-filtered sample was low, although several bands were recognized as being able to produce filaments. The relative importance of the β-*Proteobacteria* group increased in the filament samples, rising to 87% of the total signal in Lake Mascardi at T_{72} under the 50% UVR + PAR treatment (71% and 49% in Gutiérrez and Correntoso, respectively).

DISCUSSION

The results of our laboratory experiments demonstrate a positive response as regards increased filament formation and

Table 4. Jaccard similarity index matrices comparing the presence of OTU at the beginning of the experiment (T_0) and after 72 h for each treatment (UVR + PAR50%, UVR + PAR, PAR50% and PAR).

	Gutiérrez			
	UVR + PAR50%	UVR + PAR	PAR50%	PAR
T_0	0.81	0.81	0.81	0.81
UVR + PAR50%		1.00	1.00	1.00
UVR + PAR			1.00	1.00
PAR50%				1.00
	Mascardi			
	UVR + PAR50%	UVR + PAR	PAR50%	PAR
T_0	0.77	0.77	0.74	0.74
UVR + PAR50%		1.00	0.96	0.96
UVR + PAR			0.96	0.92
PAR50%				1.00
	Correntoso			
	UVR + PAR50%	UVR + PAR	PAR50%	PAR
T_0	0.90	0.90	0.81	0.81
UVR + PAR50%		1.00	0.89	0.89
UVR + PAR			0.89	1.00
PAR50%				1.00

OTU = operational taxonomic unit; UVR = UV radiation; PAR = photosynthetically active radiation.

filament length (and, consequently, higher cell biovolume) within bacteria assemblages under UVR + PAR exposure. Cell filamentation is a well-known process that can be induced by the "SOS response" through the activation of a pool of specific genes after various physical or chemical treatments, including exposure to strong UVR, that damage or inhibit DNA replication (18). As the samples for our experiments were obtained at 1% of the UV-A 340 nm band, where the proportion of filaments was negligible (≤1%), it could be argued that the observed increase in filamentation is a physiological response of naïve bacteria to harsh conditions generated in the experimental UVR treatment. In this sense, Abboudi *et al.* (15) found that filamentation in *Vibrium angustum* was induced by UV-B but not by UV-A or visible light. However, our experiments demonstrate that bacteria are able to react to moderate doses of UVR (50% UVR + PAR treatment = 15 μW cm^{-2} nm^{-1} of the 340 nm band, *i.e.* equivalent to mean epilimnetic summer sunlight in Andean lakes and 3 μW cm^{-2} nm^{-1} of the 305 nm band), and these exposure levels are enough to drive morphological changes in bacterial communities. The percentage of bacterial filament biovolume obtained in the 50% UVR + PAR treatment (47%) are similar to those observed in Andean lakes (up to 57%), suggesting that UVR exposure in nature and in the laboratory has comparable effects in producing bacterial filaments. In addition, the positive filament formation response observed under UVR exposure shows that the bacterial assemblages of the deep epilimnion and metalimnion (1% of the UV-A 340 nm band) have the potential to develop into filaments. As the samples for our experiments were obtained early in the stratification season (November 2008), changes in the thermocline level could occur (33). Thus, the original metalimnetic community may be exposed to epilimnetic UVR levels in the summer. A recent study of Andean lakes in mid-summer by Corno *et al.* (19) indicated that there was no bacterial strain segregation between the epilimnion, metalimnion and hypolimnion; it can therefore be proposed that, if bacteria in the epilimnion can develop into filaments, those in deeper layers should also be capable of doing so.

Bacterial filament formation can occur in the absence of predation when bacteria grows in C-rich but inorganic nutrient-poor environments (34). As UVR modifies the DOM that can affect bacterial growth (35–37), it could be argued that the observed results are the outcome of the changes in DOM. However, DOC concentrations in the three lakes included in our experiments are extremely low (< 50 μM) (24), and the addition of organic carbon as cycloheximide did not modify these original low values ($< 10\%$ increase). The interaction experiment indicated that the use of cycloheximide at a low concentration (100 μg L^{-1} final concentration) does not induce filamentation, either by itself or in interaction with UVR. Although this concentration was sufficient to reduce nanoflagellates, it did not produce the negative effects on bacteria observed at higher concentrations of cycloheximide (38). We used the lowest concentration of cycloheximide within the range reported in the literature (38,39) and our finding highlights the importance of the use of concentration thresholds to achieve the requirements of a good selective inhibitor.

During the experiments, the DOC : total dissolved phosphorus atomic ratio remained constant (around 500) in all treatments. Also, the spectrophotometric scans did not vary during the 72 h of the experiment; we can therefore assume that photobleaching was negligible in these waters with low DOC concentrations. Similarly, other authors have reported very low levels of photobleaching in water in large, deep Andean lakes, with no measurable changes in DOM (27). Therefore, the filamentation observed in our experiments cannot result from changes in DOM and nutrient supply. Thus, we were able to demonstrate in our laboratory experiments that bacterial filament formation can be promoted by light conditions, in the absence of predators and with no changes in organic or inorganic nutrients.

Genetic analyses of the filament fraction in the experiments showed that, although only a few bands were recognized as being able to produce filaments, these bands were spread among a variety of bacterial groups, indicating that filamentation is not cluster-specific. Filamentation was observed in various members of the *γ-Proteobacteria*, *α-Proteobacteria*, *β-Proteobacteria* and CFB. *Actinobacteria* seems to be the only bacterial group with a very weak filamentation response (only one band in one lake was recognized). However, this group has been mentioned as being very resistant to UVR (40), suggesting that alternative strategies to overcome this stress factor exist. The CFB group has a well-known tendency toward filamentation (4), especially under high grazing pressure (1). In our experiments, we were also able to identify that OTUs belonging to the CFB group were capable of producing filaments under UVR exposure, along with *β-Proteobacteria*.

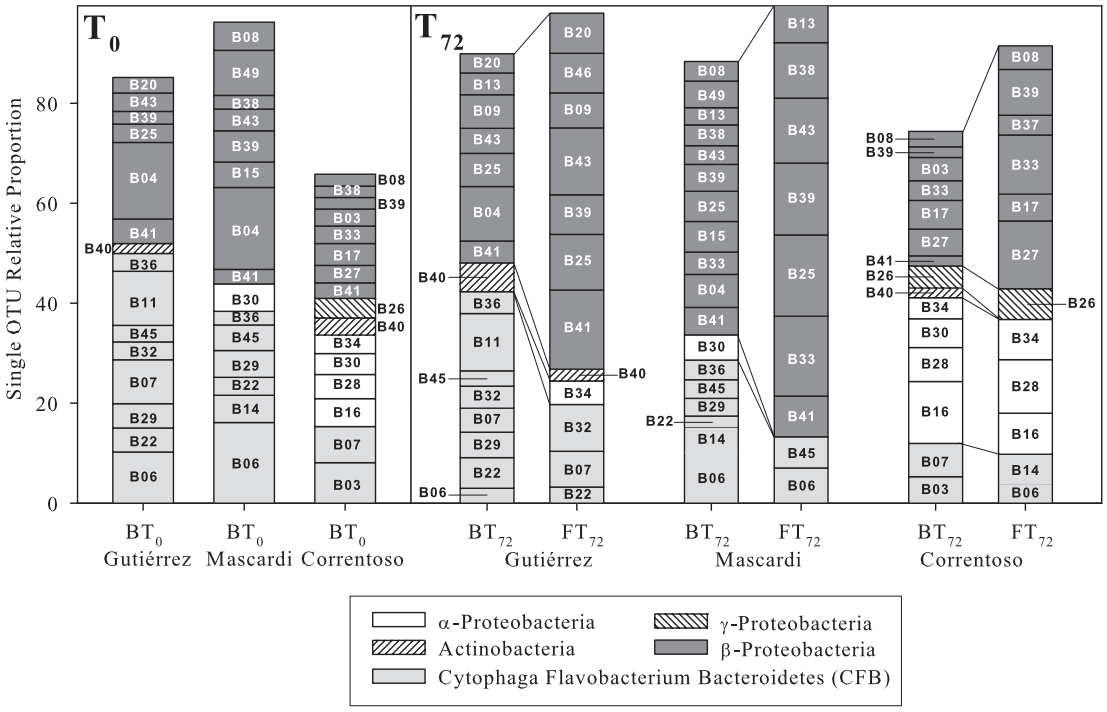

Figure 3. Relative proportions of operational taxonomic units (OTUs) measured in laboratory experiments at T_0 and at T_{72} for each lake in the 50% UVR + PAR treatments, for the whole bacterial community (BT_0 and BT_{72}) and for the fraction >5 μm (filaments, FT_{72}); only OTUs positively sequenced and accounting for more than 3% in at least one treatment were considered. For each OTU the closest known sequence available in GenBank has been selected as follows (band nr.: closest sequence name [GenBank accession number, % identity, % coverage]): B03: Uncultured *Flavobacterium* sp. (DQ628917, id: 99, cov: 96); B04: *Burkholderiales* bact. (EF636126, id: 97, cov: 100); B06: uncultured Bacteroidetes (FJ532605, id: 94, cov: 90); B07: *Flavobacterium* sp. (FJ447544, id: 98, cov: 100); B08: β-proteobact. (several sequences, id: 99, cov: 100); B09: uncultured *Bacillus* sp. (EU567044, id: 96, cov: 99); B11: uncultured Flavobacteriaceae (EU640043, id: 96, cov: 99); B13: β-proteobact. (several sequences id: 99, cov: 99); B14: Bacteroidetes (several sequences id: 99, cov: 100); B15: uncultured Comamonadaceae (EF562102, id: 92, cov: 99); B16: *Brevundimonas* sp. (AB426562, id: 99, cov: 99); B17: uncultured Methylophilaceae (EU639968, id: 92, cov: 100); B20: denitrifying bacterium (AB162105, id: 90, cov: 98); B22: *Candidatus Aquirestis calciphila* (AJ786331, id: 94, cov: 99); B25: uncultured *Aquabacterium* sp. (EU706220 id: 97, cov: 99); B26: *Nevskia* sp. (AB426558, id: 90, cov: 99); B27: uncultured Burkholderiales (EU640623, id: 97, cov: 99); B28: *Sphingomonas* sp. (FJ626798, id: 96, cov: 94); B29: *Candidatus Aquirestis calciphila* (AJ786335, id: 98, cov: 95); B30: *Sphingomonas* sp. (EU741013, id: 98, cov: 89); B32: Flavobacteria (several sequences, id: 100, cov: 100); B33: *Comamonas* sp. (several sequences, id: 99, cov: 100); B34: α-proteobact. (several sequences, id: 99, cov: 100); B36: uncultured Flavobacteriaceae (EU642223, id: 97, cov: 90); B37: *Comamonas* sp. (several sequences, id: 100, cov: 99);B38: β-proteobact. (several sequences, id: 100, cov: 100); B39: β-proteobact. (EF626687, id: 97, cov: 99); B40: Actinobacteria (EU642093, id: 99, cov: 99); B41: *Burkholderiales* bacterium (EF636126, id: 97, cov: 99); B43: β-proteobact. (EF626687 id: 95, cov: 99); B45: Flavobacteria (several sequences id: 99, cov: 100); B46: β-proteobact. (several sequences, id: 99, cov: 99); B49: β-proteobact. (several sequences, id: 98, cov: 100).

The evidence we obtained in the laboratory, together with the results from field studies (19), shows that UVR can promote bacterial community heterogeneity by increasing the filamentation of certain bacteria groups. Because of this, UVR can cause a decrease in the bacterial biovolume available for nanoflagellate grazing. In this scenario, predators encounter a prey assemblage composed mainly (on average 36% of biovolume) of inedible prey (19) greatly reducing the probability of reaching available prey. Thus, UVR indirectly reduces bacterivory and energy transfer to upper trophic levels, as a high proportion of bacterial carbon becomes unavailable for nanoflagellates in the epilimnion of highly transparent lakes. It has been argued that as filamentation depends on available substrates and cell growth rate, and aquatic bacteria exhibit low growth rates, the UVR effect on filamentation would be expected to be less important in nature, being insufficient to form long filaments (15). However, in Andean lakes we found that filament length in the epilimnion was on average 20 μm in length. This result indicates that in these transparent lakes the mean irradiance of UVR in the epilimnion is effective in inducing filament formation (19). Thus, UVR would effectively reduce protist bacterivory, as filament formation did occur.

Besides the eventual advantage of reducing top-down effects, does the production of filaments produce any other gains for bacteria? UVR damages bacterial DNA, inducing pyrimidine dimers (41,42), and also induces filament formation. It has been proposed that cellular aggregation enhances DNA transfer among *Sulfolobus* cells, promoting the repair of damaged DNA *via* homologous recombination (43). The filament formation observed in our experiments would provide an advantage under UVR stress, as filaments have multiple copies of DNA (15). Because the probability of UVR damage in the same locus of different copies is negligible, DNA repair *via* homologous recombination can be very efficient within a filament as there are many copies of DNA in close proximity (43). Therefore, filamentation with multiple copies of DNA should also be highly adaptive under these circumstances, as using copies of DNA within the filament avoids the need to encounter cells of the same species in multiple-species systems with very low cell

abundance. The inhibition of cell division, and hence of filamentation, protects the daughter cells from receiving damaged DNA, and when DNA repair is complete, cell division capacity is restored (18). Therefore, filamentation should enhance the survival of bacterial cells under UVR stress and ensure DNA repair in daughter cells. This response would be especially important in Andean lakes where UVR penetrates deeply into the epilimnion (25), so depth in the epilimnion may not by itself provide a refuge against this factor.

Acknowledgements—We thank Elisa Peters for English writing assistance. This work was carried out as part of an International Cooperation Program between Argentina-Italy (CONICET-CNR). It was supported by FONCyT PICT 2007-01256 and FONCyT PICT 2007-01258.

REFERENCES

1. Corno, G. and K. Jürgens (2006) Direct and indirect effects of protist predation on population size structure of a bacterial strain with high phenotypic plasticity. *Appl. Environ. Microbiol.* **72**, 78–86.
2. Jürgens, K. and C. Matz (2002) Predation as a shaping force for the phenotypic and genotypic composition of planktonic bacteria. *Antonie Van Leeuwenhoek* **81**, 413–434.
3. Sommaruga, R. and R. Psenner (1995) Permanent presence of grazing-resistant bacteria in a hypertrophic lake. *Appl. Environ. Microbiol.* **61**, 3457–3459.
4. Pernthaler, J., F. O. Glöckner, S. Unterholzner, A. Alfreider, R. Psenner and R. Amann (1998) Seasonal community and population dynamics of pelagic bacteria and archaea in a high mountain lake. *Appl. Environ. Microbiol.* **64**, 4299–4306.
5. Vrba, J., J. Nedoma, L. Kohout, J. Kopacek, L. Nedbalova, P. Rackova and K. Šimek (2003) Massive occurrence of heterotrophic filaments in acidified lakes: Seasonal dynamics and composition. *FEMS Microbiol. Ecol.* **46**, 281–294.
6. Wille, A., B. Sonntag, B. Sattler and R. Psenner (1999) Abundance, biomass and size structure of the microbial assemblage in the high mountain lake Gossenköllesee (Tyrol, Austria) during the ice-free period. *J. Limnol.* **58**, 117–126.
7. Pernthaler, J. (2005) Predation on prokaryotes in the water column and its ecological implications. *Nat. Rev. Microbiol.* **3**, 537–546.
8. Pernthaler, J., E. Zöllner, F. Warnecke and K. Jürgens (2004) Bloom of filamentous bacteria in a mesotrophic lake: Identity and potential controlling mechanism. *Appl. Environ. Microbiol.* **70**, 6272–6281.
9. Corno, G. and K. Jürgens (2008) Structural and functional patterns of bacterial communities in response to protist predation along an experimental productivity gradient. *Environ. Microbiol.* **10**, 2857–2871.
10. Corno, G., E. Caravati, C. Callieri and R. Bertoni (2008) Effects of predation pressure on bacterial abundance, diversity, and size-structure distribution in an oligotrophic system. *J. Limnol.* **67**, 107–119.
11. Hahn, M. W. and M. G. Hofle (2001) Grazing of protozoa and its effect on populations of aquatic bacteria. *FEMS Microbiol. Ecol.* **35**, 113–121.
12. Roszak, D. B. and R. R. Colwell (1987) Survival strategies of bacteria in the natural environment. *Microbiol. Rev.* **51**, 365–379.
13. Kalle, G. P. and P. P. Sivasubramanian (1967) Filament formation in ultraviolet-resistant mutants of *Escherichia coli* strain B-3. *Radiat. Res.* **30**, 71–80.
14. Witkin, E. M. (1967) The radiation sensitivity of Escherichia coli B: A hypothesis relating filament formation and prophage induction. *Proc. Natl Acad. Sci. USA* **57**, 1275–1279.
15. Abboudi, M., S. M. Surget, J. F. Rontani, R. Sempéré and F. Joux (2008) Physiological alteration of the marine bacterium *Vibrio angustum* S14 exposed to simulated sunlight during growth. *Curr. Microbiol.* **57**, 412–417.
16. Wu, H., K. Gao, V. E. Villafañe, T. Watanabe and E. W. Helbling (2005) Effects of solar UV radiation on morphology and photosynthesis of filamentous cyanobacterium *Arthrospira platensis*. *Appl. Environ. Microbiol.* **71**, 5004–5013.
17. Walker, J. R. and A. B. Pardee (1968) Evidence for a relationship between deoxyribonucleic acid metabolism and septum formation in *Escherichia coli*. *J. Bacteriol.* **95**, 123–131.
18. Justice, S. S., D. A. Hunstad, L. Cegelski and S. J. Hultgren (2008) Morphological plasticity as a bacterial survival strategy. *Nat. Rev. Microbiol.* **6**, 162–168.
19. Corno, G., B. Modenutti, C. Callieri, E. Balseiro, R. Bertoni and E. Caravati (2009) Bacterial diversity and morphology in deep ultraoligotrophic Andean lakes: The role of UVR on vertical distribution. *Limnol. Oceanogr.* **54**, 1098–1112.
20. Joux, F., W. H. Jeffrey, P. Lebaron and D. L. Mitchell (1999) Marine bacterial isolates display diverse responses to UV-B radiation. *Appl. Environ. Microbiol.* **65**, 3820–3827.
21. Fernandez Zenoff, V., J. Heredia, M. Ferrero, F. Siñeriz and M. E. Farías (2006) Diverse UV-B resistance of culturable bacterial community from high-altitude wetland water. *Curr. Microbiol.* **52**, 359–362.
22. Alonso-Sáez, L., J. M. Gasol, T. Lefort, J. Hofer and R. Sommaruga (2006) Effect of natural sunlight on bacterial activity and differential sensitivity of natural bacterioplankton groups in Northwestern Mediterranean coastal waters. *Appl. Environ. Microbiol.* **72**, 5806–5813.
23. Kataoka, T., Y. Hodoki, K. Suzuki, H. Saito and S. Higashi (2009) Detection of UVBR-sensitive and -tolerant bacteria in surface waters of the western North Pacific. *J. Photochem. Photobiol.* **95**, 108–116.
24. Morris, D. P., H. Zagarese, C. E. Williamson, E. G. Balseiro, B. R. Hargreaves, B. Modenutti, R. Moeller and C. Queimaliños (1995) The attenuation of solar UV radiation in lakes and the role of dissolved organic carbon. *Limnol. Oceanogr.* **40**, 1381–1391.
25. Balseiro, E., M. S. Souza, B. Modenutti and M. Reissig (2008) Living in transparent lakes: Low food P:C ratio decreases antioxidant response to ultraviolet radiation in *Daphnia*. *Limnol. Oceanogr.* **53**, 2383–2390.
26. Porter, K. G. and Y. S. Feig (1980) The use of DAPI for identifying and counting aquatic microflora. *Limnol. Oceanogr.* **25**, 943–948.
27. Osburn, C. L., H. E. Zagarese, D. P. Morris, B. R. Hargreaves and W. E. Cravero (2001) Calculation of spectral weighting functions for the solar photobleaching of chromophoric dissolved organic matter in temperate lakes. *Limnol. Oceanogr.* **46**, 1455–1467.
28. Shick, J. M., W. C. Dunlap and B. E. Chalker (1992) Survey of ultraviolet radiation-absorbing microsporine-like amino acids in organs of coral reef holothuroids. *Mar. Ecol. Progr. Ser.* **90**, 139.
29. Corno, G. (2006) Effects of nutrient availability and *Ochromonas* sp. predation on size and composition of a simplified aquatic bacterial community. *FEMS Microbiol. Ecol.* **58**, 354–363.
30. Sanchez, O., J. M. Gasol, R. Masana, J. Mas and C. Pedrós-Alió (2007) Comparison of different denaturing gradient gel electrophoresis primer sets for the study of marine bacterioplankton communities. *Appl. Environ. Microbiol.* **73**, 5962–5967.
31. Muyzer, G., T. Brinkhoff, U. Nuebel, C. Santegoeds, H. Schaefer and C. Wawer (1998) Denaturing gradient gel electrophoresis (DGGE) in microbial ecology. In *Molecular Microbial Ecology Manual* (Edited by A. D. L. Akkermans, J. D. van Elsas and F. J. Bruijn), pp. 1–27. Kluwer Academic Publishers, Dordrecht.
32. Pielou, E. C. (1984) *The Interpretation of Ecological Data. A Primer on Classification and Ordination*. John Wiley & Sons, New York.
33. Modenutti, B. E., E. G. Balseiro, C. Callieri and R. Bertoni (2008) Light versus food supply as factors modulating niche partitioning in two pelagic mixotrophic ciliates. *Limnol. Oceanogr.* **53**, 446–455.
34. Matz, C. and K. Jürgens (2003) Interaction of nutrient limitation and protozoan grazing determines the phenotypic structure of a bacterial community. *Microb. Ecol.* **45**, 384–398.
35. Obernosterer, I., B. Reitner and G. J. Herndl (1999) Contrasting effects of solar radiation on dissolved organic matter and its

bioavailability to marine bacterioplankton. *Limnol. Oceanogr.* **44**, 1645–1654.
36. Perez, M. T. and R. Sommaruga (2007) Interactive effects of solar radiation and dissolved organic matter on bacterial activity and community structure. *Environ. Microbiol.* **9**, 2200–2210.
37. Bastidas Navarro, M., E. Balseiro and B. Modenutti (2009) Effect of UVR on lake water and macrophyte leachates in shallow Andean-Patagonian lakes: Bacterial response to changes in optical features. *Photochem. Photobiol.* **85**, 332–340.
38. Tremaine, S. C. and A. L. Mills (1987) Inadequacy of the eucaryote inhibitor cycloheximide in studies of protozoan grazing on bacteria at the freshwater–sediment interface. *Appl. Environ. Microbiol.* **53**, 1969–1972.
39. DeLorenzo, M. E., A. J. Lewitus, G. I. Scott and P. E. Ross (2001) Use of metabolic inhibitors to characterize ecological interactions in an estuarine microbial food web. *Microb. Ecol.* **42**, 317–327.
40. Warnecke, F., R. Sommaruga, R. Sekar, J. S. Hofer and J. Pernthaler (2005) Abundances, identity, and growth state of Actinobacteria in mountain lakes of different UV transparency. *Appl. Environ. Microbiol.* **71**, 5551–5559.
41. Mitchell, D. L. and D. Karentz (1993) The induction and repair of DNA photodamage in the environment. In *Environmental UV Photobiology* (Edited by A. R. Young, L. O. Bjorn, J. Moan and W. Nultsch), pp. 345–377. Plenum Press, New York.
42. Hernández, K. L., R. A. Quiñones, G. Daneri, M. E. Farias and E. W. Helbling (2007) Solar UV radiation modulates daily production and DNA damage of marine bacterioplankton from a productive upwelling zone (36°C), Chile. *J. Exp. Mar. Biol. Ecol.* **343**, 82–95.
43. Fröls, S., M. Ajon, M. Wagner, D. Teichmann, B. Zolghadr, M. Folea, E. J. Boekema, A. J. M. Driessen, C. Schleper and S. V. Albers (2008) UV-inducible cellular aggregation of the hyperthermophilic archaeon *Sulfolobus solfataricus* is mediated by pili formation. *Mol. Microbiol.* **70**, 938–952.